Asian Congress of Structural and Multidisciplinary Optimization 2020
Korea, 22-26 November 2020

Paper No. 00047

Topology Optimization for Part Consolidation Considering the Tradeoff Between Support Volume and Joining Costs

Luke Crispo[1], Il Yong Kim[1*]

[1]*Department of Mechanical and Materials Engineering, Queen's University, Kingston, ON, Canada*

Abstract

As additive manufacturing continues to see increased adoption in the aerospace industry, part consolidation is becoming a viable cost savings approach. Current research is focused on reducing the total number of parts in an assembly, instead of reducing overall cost. This work presents a novel topology optimization approach for assembly design that models parts using multiple overlapping design domains occupying the same physical space and determines the ideal connection layout between parts with a joining domain. A multi-objective problem statement minimizes the weighted sum of structural compliance and the overall cost of the part, considering support structure volume and the number of joints in the assembly. The methodology is applied on an academic example, demonstrating the complex relationship between additive manufacturing printing cost and joining cost.

Keywords: Part consolidation, Design for additive manufacturing, Multicomponent topology optimization, Multi-layered approach

1. Introduction

Topology optimization (TO) is a design generation tool that uses a mathematical formulation to maximize performance subject to specified constraints. Additive manufacturing (AM) can easily print the complex designs generated by TO due to the near unlimited design freedom possible when building a part layer-by-layer. There has been significant research dedicated to the integration of AM factors, such as reduction of support structure requirements or selection of ideal build orientation, into topology optimization algorithms [1-3].

Part consolidation (PC) leverages AM to print several parts in an assembly as a single piece, reducing joining costs and often improving performance. Current research in PC has focused on a top-down approach that uses the baseline assembly as a starting point and combines parts together followed by a part redesign [4, 5]. These approaches have a limited number of part combinations and therefore remove design freedom from the part consolidation process. A bottom-up approach, such as one proposed Zhou et al. [6] or Crispo and Kim [7], instead starts from the original design space and divides it into parts, resulting in an unlimited number of part combinations. This improves design freedom over the top-down approach and can generate improved designs that would not be possible with a top-down approach.

Previous part consolidation approaches attempt to minimize the total number of parts in an assembly. Some factors can prevent an assembly from being consolidated into a single part, such the maximum size limit of the printing build plate or relative motion requirements as defined by Yang et al [8]. However, there is also a trade-off between part cost and assembly cost as the number of parts decreases [9] that is not considered in current PC research. As the number of parts in an assembly decreases (and the associated assembly cost is reduced), the complexity of the remaining parts increases. This may increase printing costs due to larger support structure volume and printing time. The trade-off between these costs is demonstrated on a simple geometry in Fig. 1 (assuming the part orientation is fixed). The single part has no assembly cost but a high printing cost, whereas the multiple-part design has a high assembly cost but low printing costs. Based on the relative differences between these costs, an optimal number of parts can be determined that decreases the overall cost of the assembly.

The objective of this work is to present a novel TO algorithm using a bottom-up approach for assembly design. The complex trade-off between assembly cost and AM part cost will be mathematically integrated into the optimization problem statement to determine the optimal number of parts to consolidate, along with the ideal part geometry and joining pattern. Assembly cost will be represented as the total number of joints in the assembly and AM part cost will be approximated by the volume of support structure required.

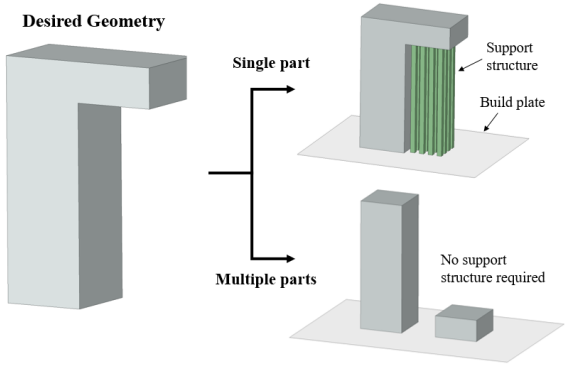

Fig. 1. Trade-off between support structure and assembly cost demonstrated on a simple example.

*Corresponding author. Tel.: (613) 533-3077
E-mail address: kimiy@queensu.ca

2. Methodology

2.1 Assembly Level Topology Optimization

The bottom-up optimization of an assembly requires the extension of traditional single-part topology optimization formulations to consider the design of multiple parts and their connections. A multi-layered approach, conceived by Crispo and Kim [7], is used as the foundation for the part consolidation methodology in this work. In this approach, the geometry of each part is defined using L overlapping part domains with identical finite element meshes, where the design variable vector $\underset{\sim}{x}$ controls the existence of elements within each domain. The connection pattern is determined through the accompanying joint domain, with the design variable $\underset{\sim}{y}$ controlling the existence of joints at each node in the assembly domain. This layered approach is demonstrated in Fig. 2 for 2D with an expanded view of all domains for visualization purposes.

Element densities may vary between 0 (void) and 1 (solid) with the elastic modulus of each element interpolated using the solid isotropic material with penalization (SIMP) method as follows:

$$\begin{aligned} E_e\left(x_e\right) &= E_{\min} + x_e^{\,p}\left(E_0^1 - E_{\min}\right) \\ E_j\left(y_j\right) &= E_{\min} + y_j^{\,q}\left(E_0^2 - E_{\min}\right) \end{aligned} \tag{1}$$

where $E_e\left(x_e\right)$ and $E_j\left(y_j\right)$ represent the stiffness of the e-th element and j-th joint respectively, $E_{\min}$ represents a non-zero minimum stiffness value, p and q denote the element and joint penalty factors, E_0^1 is the Young's modulus of the part material, and E_0^2 is the base joint stiffness. The base joint stiffness has units of [N/m] and can be calculated using fastener models such as those developed by Douglas or Huth [10].

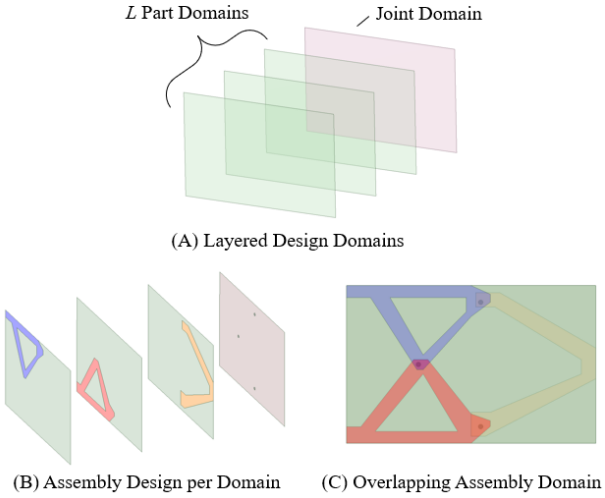

Fig. 2. Layered design domain approach presented in 2D with examples from a simple assembly design.

The global stiffness matrix of the assembly, $\underset{\sim}{K}$, is calculated as the sum of all element and joint stiffness matrices as:

$$\underset{\sim}{K} = \sum_{e=1}^{N} E_e\left(x_e\right)\underset{\sim}{K}_e^0 + \sum_{j=1}^{M}\left(E_j\left(y_j\right)\sum_{c=1}^{L-1}\underset{\sim}{K}_c^0\right) \tag{2}$$

where $\underset{\sim}{K}_e^0$ is the element level stiffness matrix and $\underset{\sim}{K}_c^0$ is the sub-joint level stiffness matrix. The element stiffness matrices are summed over N total elements. Joint stiffness matrices are first summed over $L-1$ connections between domains at a single nodal location followed by a summation over M total joint locations in the assembly.

A sub-joint is built from the summation of a set of bar elements connecting between domains for each of the spatial degrees of freedom in the model. Each sub-joint connects two part domains. The stiffness matrix of each bar element is modified by setting the cross-sectional area A, the Young's Modulus E, and the length l equal to a value of unity as the joint stiffness is calculated using Eq. (1). The sub-joint level stiffness matrix is therefore equal to:

$$\left[\underset{\sim}{K}_c^0\right] = \begin{bmatrix} \underset{\sim}{I} & \cdots & -\underset{\sim}{I} \\ \vdots & \ddots & \vdots \\ -\underset{\sim}{I} & \cdots & \underset{\sim}{I} \end{bmatrix} \tag{3}$$

where $\underset{\sim}{I}$ is the identity matrix with a dimension equal to the number of spatial dimensions. The innermost summation of Eq. (2) over each c connection is required when more than two part domains are used ($L > 2$). In this case, sub-joints are placed from the node in the part domain with the largest element density to nodes in all other part domains. This sub-joint placement results in consistent modelling of joints between domains while also allowing for emerging density to develop in new locations during optimization.

The assembly cost can be approximated by the summation of all joint design variable densities as:

$$\Gamma = \sum_{j=1}^{M} y_j \tag{4}$$

where Γ is the total number of joints in the assembly. While this value can be used as a representation for joining cost, it is not the true number of physical joints in the assembly because joints can be placed unrealistically close at every node. An interpretation of the optimization results would be required to group several joint elements into a realistic joint design.

2.2 Support Volume Calculation

The required support structure volume can be used as an approximation of the AM printing cost following the methodology developed by Ryan and Kim [11]. This approach uses the Helmholtz PDE filter [12] to enforce smooth part boundaries to aid in interface detection. Element design variables are con-

verted to nodal densities, then filtered using with the Helmholtz PDE, and finally converted to filtered element densities.

The spatial gradient of the element densities, $\nabla\rho_e$, can be calculated for each part domain as:

$$\nabla\rho_e = \sum_{k=1}^{N_d} \underset{\sim}{B}_e^k \tilde{\rho} \hat{e}_k \tag{5}$$

where N_d is the number of spatial dimensions, $\underset{\sim}{B}_e^k$ represents the strain-displacement matrix of the *e*-th element in the *k*-th direction, $\tilde{\rho}$ is the vector of nodal filtered densities, and $\hat{e}_k$ is a unit vector in the *k*-th direction. The spatial gradient of each element is a vector that points in the direction of increasing element density.

The surface condition number, Φ_e, and the supported surface condition number, ψ_e, can be calculated as per Eq. (6). The surface condition number identifies if an element is located on the boundary of the part geometry, while the supported surface number determines if an element is overhanging and requires support structure. The supported surface number is calculated using the dot product of the normalized spatial gradient and the build direction vector, $\hat{b}$ (which can be uniquely defined for each part domain). This value is then thresholded using the smooth Heaviside function $H_{\bar{\alpha}}(\square)$ defined by Qian [13] using a self-supporting threshold angle $\bar{\alpha}$ of 45 degrees. Multiplying by the surface condition number ensures supported elements only occur at the boundary of each part geometry.

$$\begin{aligned} \Phi_e &= \left\|\nabla\rho_e\right\| \\ \psi_e &= H_{\bar{\alpha}}\left(\frac{\nabla\rho_e}{\left\|\nabla\rho_e\right\|}\cdot\hat{b}\right)\Phi_e \end{aligned} \tag{6}$$

The support structure volume associated with each supported element, λ_e, is calculated using integral along a $\vec{z}_i$ ray (oriented in the $-\hat{b}$ direction originating at the supported element) as shown in Eq. (7). The upper integrating limit of the integral, b_e, represents the t position associated with the supported element along the ray. The lower integrating limit, a_e, represents the t position of the first surface element along the ray or the build plate of the part domain. Discrete locations for integration limits are calculated using a peak finding algorithm. Support structure volume is dependent on element volumes, $\underset{\sim}{V}$, and the densities of elements below each supported element. The total support structure volume, Λ, required to print the assembly is calculated as the sum of all individual element support structure.

$$\begin{aligned} \Lambda &= \sum_{e=1}^{N} \lambda_e \\ \lambda_e &= \int_{a_e}^{b_e} \underset{\sim}{V}\left(\vec{z}_i(t)\right)\left(1-\underset{\sim}{\rho}\left(\vec{z}_i(t)\right)\right)dt \end{aligned} \tag{7}$$

2.3 Optimization Problem Statement

The optimization problem statement of the proposed part consolidation methodology is stated in Eq. (8), where the objective function is the minimization of the weighted sum between global compliance, C, total number of joints, Γ, and total support structure volume, Λ. All objective responses are normalized based on their magnitude in the first iteration (C_0, Γ_0, Λ_0). Weighting factors w_1 and w_2 are defined as the structural-cost weighting and joint-part cost weighting respectively.

$$\begin{aligned} \min:\ & w_1\frac{C\left(\underset{\sim}{x},\underset{\sim}{y}\right)}{C_0} + \left(1-w_1\right)\left(w_2\frac{\Gamma\left(\underset{\sim}{y}\right)}{\Gamma_0} + \left(1-w_2\right)\frac{\Lambda\left(\underset{\sim}{x}\right)}{\Lambda_0}\right) \\ \text{s.t.:}\ & \underset{\sim}{K}\underset{\sim}{u} = \underset{\sim}{f} \\ & \sum_{e=1}^{N} x_e V_e \le \gamma V_0 \\ & 0 \le x_e \le 1 \ \ \forall e \in \Omega \\ & 0 \le y_j \le 1 \ \ \forall j \in \Omega \\ & 0 \le w_i \le 1 \ \ \text{i=1,2} \end{aligned} \tag{8}$$

The optimization is subject to a linear static structural governing equation where $\underset{\sim}{u}$ is the vector of nodal displacements and $\underset{\sim}{f}$ is the vector of applied forces. A volume fraction constraint is applied with γ representing the volume fraction upper limit and V_0 as the total volume of the design space (not the sum of each part domain's volume). Design variables and the user-input weighting factors are limited between zero and unity.

3. Numerical Example

To demonstrate the effectiveness of the proposed algorithm, the approach was implemented in a custom MATLAB code using Svanberg's MMA optimizer [14]. A 2D cantilevered beam load case shown in Fig. 3 (A) was optimized using a volume fraction of 40% with 4 layered part domains. The blue lines in Fig. 3 (B) represent the build plate of each part domain with the red arrows demonstrating the build direction vector. The geometry was discretized into 250 x 100 square elements with a length of 1mm. The material Young's modulus was defined as 200 GPa, the base joint stiffness as 2000 kN/m, and the Poisson's ratio as 0.3. An adaptive penalty scheme was implemented with the element penalty factor increased from 3 to 5 after a 2% convergence was observed in all objective functions. The joint penalty factor was held constant at 3 and joint densities were initialized with a value of 0.1.

The multi-layered topology optimization approach required modification of the standard TO problem initialization to generate meaningful results. Single point constraints were applied to all part domains for the entirety of the optimization. The applied force shown in Fig. 3 (A) was split between part domains proportional to the ratio of element density in each domain at the

force location. The magnitude of force in each domain was updated during the first 3 iterations based on this density ratio. The full magnitude of the force was placed in the domain with the largest element density at the force location after iteration 3 and stayed constant for the remainder of the optimization. Element densities were initialized uniquely for each domain using smooth gradients shown in Fig. 3 (B), with a higher density at one corner of the design domain transitioning to low density at the other corner of the design domain. Overall, every design domain was initialized with an equivalent proportion of material and each location (from the assembly perspective) was initialized with an equivalent amount of material. This approach allowed material to form anywhere within the design space but provided a bias to form unique parts between part domains. Readers are referred to the work of Crispo and Kim [7] for more details on problem initialization.

The cantilever beam load case was optimized for a sweep of structural-cost weightings (w_1) between 0.40 – 0.95 and joint-part cost weightings (w_2) between 0.01 – 1.00. In addition to the parameter sweep, a baseline single part was optimized with $w_1 = 0.99$ and $w_2 = 1.00$ while a baseline assembly was optimized using $w_1 = 0.99$ and $w_2 = 0.5$. All objective function values presented in the following figures were normalized towards the baseline single part design except for joints which are normalized with reference to the baseline assembly.

The baseline optimization results are presented in Fig. (4) showing the baseline single part design and the baseline assembly design, both with minimal weightings applied to cost minimization. Calculated support structure volume is graphically represented in red with joints plotted as red or green stars. The baseline assembly reduces support volume by 47 % by splitting the original part into several less complex parts and leveraging the different print orientations of each domain. The compliance of the baseline assembly is larger than the baseline single part because the connections through joints are less stiff than a single uniform part.

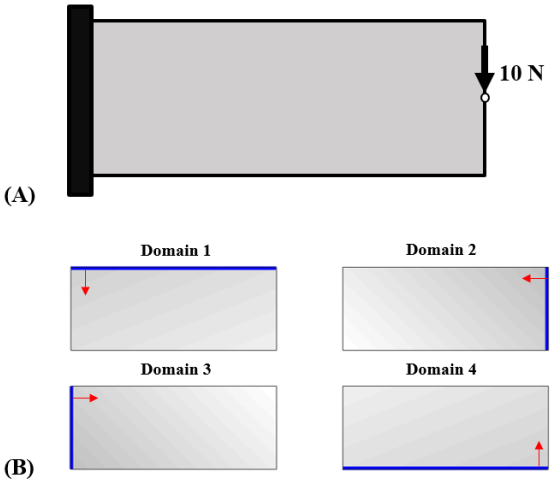

Fig. 3. (A) Cantilever beam load case and (B) element density initialization and build direction vector per part domain.

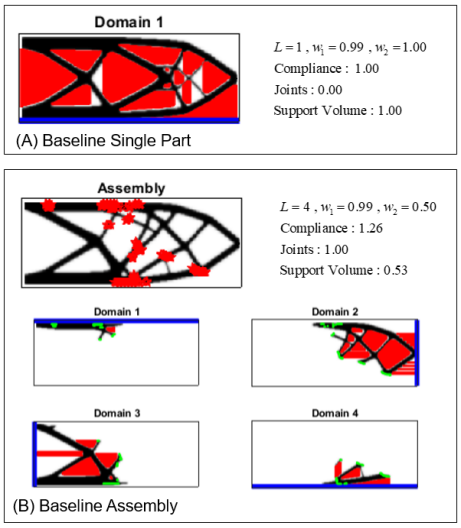

Fig. 4. Optimization results for (A) the baseline single part and (B) the baseline assembly design.

Two optimized designs are presented in Fig. (5) with a focus on minimizing the number of joints in the assembly in (A) and minimizing the total support structure volume in (B). The optimization produces a single part design when a large weighting factor is applied to joint minimization. Note that a single part design is possible even when starting with four layered domains. The compliance and support structure volume are approximately 5% greater than the baseline single part due to convergence to a local minimum from the initial density distribution. The "Reducing Support Volume" design decreases support structure by an additional 26% over the baseline assembly by "pulling" the part geometry towards the build plate. In addition, the number of joints is reduced by 47% and compliance is increased by 73% over the baseline assembly.

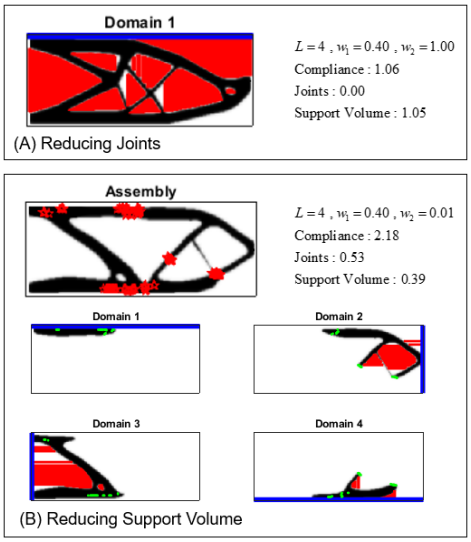

Fig. 5. Optimization results for (A) weighting factors focused on reducing joints and (B) weighting factors focused on reducing support volume.

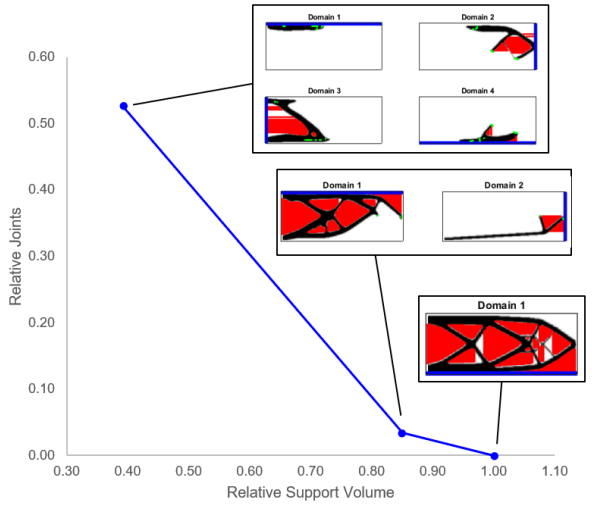

Fig. 6. Plot of relative joints and support volume for select designs from the parameter sweep.

Fig. 6 demonstrates the relationship between joints and support structure volume that was outlined as the focus of this work. A decrease in the number of parts and joints in the design was accompanied by an approximately two-fold increase support structure requirements. By capturing this trade-off between printing cost and assembly cost during part consolidation, designers can minimize the overall cost of the assembly (instead of only the joining cost).

The relationship between compliance and support structure volume is presented for Fig. 7 for a series of designs from the parameter study. Support structure volume and compliance were conflicting objectives in the optimization. A decrease in support structure volume must be accompanied by an increase in compliance either through a change in part topology that reduces support structure but decreases stiffness, or an increase in the number of parts that reduces stiffness but decreases part complexity and printing time.

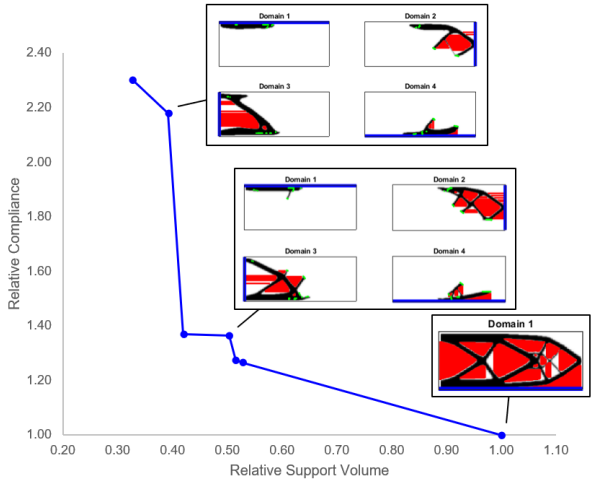

Fig. 7. Plot of relative compliance and relative support volume for select designs from the parameter sweep.

4. Conclusions

This work presented a part consolidation approach for the design optimization of assemblies using additive manufacturing. A multi-objective approach was implemented to reduce the weighted trade-off between structural compliance, total number of joints, and total support structure volume. The ideal number of parts, part geometry, and connection pattern was selected through a bottom-up TO methodology that minimized the overall cost of the assembly. Application to a cantilever beam problem demonstrated that support volume and joining costs are conflicting objectives, and that the trade-off between objective responses varied based on user-input weighting factors. Future work includes the extension to 3D geometries with complex loading, the optimization of ideal build orientation through an added design variable, and the consideration of other AM factors such as build plate size or removal of internal voids.

Acknowledgment

This work supported by the National Sciences and Engineering Research Council of Canada (NSERC).

Nomenclature

x_e / y_j : Element/Joint design variable
E_e / E_j : Interpolated element stiffness
p / q : Element / join penalty factor
E_0^1 : Material Young's modulus
E_0^2 : Base joint stiffness
$\underset{\sim}{K}$: Global stiffness matrix
$\underset{\sim}{K}_e^0$ / $\underset{\sim}{K}_c^0$: element / sub-joint level stiffness matrix
Γ : Total number of joints
ρ / $\tilde{\rho}$: Element / nodal filtered density
Φ_e / ψ_e : Surface / supported surface condition number
$\hat{b}$: Build direction vector
λ_e / Λ : Element / global support structure volume
V_e : Element volume
C : Structural compliance

References

[1] J. K. Liu, et al., Current and future trends in topology optimization for additive manufacturing. *Structural and Multidisciplinary Optimization*, 57 (6) (2018) 2457-2483.

[2] G. Sabiston and I. Y. Kim, 3D topology optimization for cost and time minimization in additive manufacturing. *Structural and Multidisciplinary Optimization*, 61 (2) (2020) 731-748.

[3] J. Olsen and I. Y. Kim, Design for additive manufacturing: 3D simultaneous topology and build

orientation optimization. *Structural and Multidisciplinary Optimization*, (2020).

[4] S. Yang, Y. L. Tang, and Y. F. Zhao, A new part consolidation method to embrace the design freedom of additive manufacturing. *Journal of Manufacturing Processes*, 20 (2015) 444-449.

[5] T. Reiher, et al., Holistic approach for industrializing AM technology: from part selection to test and verification. *Progress in Additive Manufacturing*, 2 (1) (2017) 43-55.

[6] Y. Zhou, T. Nomura, and K. Saitou, Multicomponent Topology Optimization for Additive Manufacturing With Build Volume and Cavity Free Constraints. *Journal of Computing and Information Science in Engineering*, 19 (2) (2019).

[7] L. Crispo and I. Y. Kim, Assembly Level Topology Optimization Towards a Part Consolidation Algorithm for Additive Manufacturing. *Proc. of AIAA Scitech 2020 Forum*, Florida, USA (2020).

[8] S. Yang, F. Santoro, and Y. F. Zhao, Towards a Numerical Approach of Finding Candidates for Additive Manufacturing-Enabled Part Consolidation. *Journal of Mechanical Design*, 140 (4) (2018).

[9] Y. Oh, C. Zhou, and S. Behdad, Part decomposition and assembly-based (Re) design for additive manufacturing: A review. *Additive Manufacturing*, 22 (2018) 230-242.

[10] S. Chandregowda and G. R. C. Reddy, Evaluation of Fastener Stiffness Modelling Methods for Aircraft Structural Joints. *Proc. of Advances in Mechanical Design, Materials and Manufacture*, India (2018).

[11] L. Ryan and I. Y. Kim, A multiobjective topology optimization approach for cost and time minimization in additive manufacturing. *International Journal for Numerical Methods in Engineering*, 118 (7) (2019) 371-394.

[12] A. Kawamoto, et al., Heaviside projection based topology optimization by a PDE-filtered scalar function. *Structural and Multidisciplinary Optimization*, 44 (1) (2011) 19-24.

[13] X. P. Qian, Undercut and overhang angle control in topology optimization: A density gradient based integral approach. *International Journal for Numerical Methods in Engineering*, 111 (3) (2017) 247-272.

[14] K. Svanberg, The Method of Moving Asymptotes - a New Method for Structural Optimization. *International Journal for Numerical Methods in Engineering*, 24 (2) (1987) 359-373.